Nickel Cobalt Thiospinel Nanoparticles as Hydrodesulfurization Catalysts: Importance of Cation Position, Structural Stability and Sulfur Vacancy

Kun Guo[a,b], Yi Ding[c], Jun Luo[c], and Zhixin Yu[a,b]*

[a] *Department of Energy and Petroleum Engineering, University of Stavanger, 4036 Stavanger, Norway*

[b] *The National IOR Centre of Norway, University of Stavanger, 4036 Stavanger, Norway*

[c] *Institute for New Energy Materials & Low-Carbon Technologies, School of Materials Science and Engineering, Tianjin University of Technology, Tianjin 300384, China*

*Corresponding author:

Zhixin Yu:

Tel.: +47 51 83 22 38;

Fax: +47 51 83 20 50;

E-mail: zhixin.yu@uis.no

Table S1. Detailed amounts of metal precursors, sulfur and oleylamine for the synthesis of different sulfides.

Sulfide sample	Metal precursors				Sulfur	Oleylamine
	$Ni(acac)_2$	$Co(acac)_3$	$Cu(acac)_2$	$Fe(acac)_3$		
NiS	1.5 mmol				1.5 mmol	15 mL
Co_3S_4		1.4 mmol			1.4 mmol	15 mL
$NiCo_2S_4$	0.5 mmol	1.0 mmol			2.0 mmol	15 mL
$CoNi_2S_4$	1.0 mmol	0.5 mmol			2.0 mmol	15 mL
$CuCo_2S_4$		1.0 mmol	0.5 mmol		2.0 mmol	15 mL
$NiFe_2S_4$	0.5 mmol			1.0 mmol	2.0 mmol	15 mL

Table S2. Elemental contents in atomic percentage derived from the XPS analysis.

Samples	Elemental content (atom %)		
	Ni	**Co**	**S**
NiS	47.5	—	52.5
Co_3S_4	—	41.4	58.6
$CoNi_2S_4$	14.4	27.2	58.4
$NiCo_2S_4$	13.6	27.5	58.9

Table S3. Elemental contents in atomic percentage derived from the XPS analysis.

Samples	Elemental content (atom %)		
	Ni	**Co**	**S**
$NiCo_2S_4$@180 °C	12.3	21.7	66.0
$NiCo_2S_4$@200 °C	10.6	21.4	68.0
$NiCo_2S_4$@230 °C	13.6	27.5	58.9
$NiCo_2S_4$@250 °C	14.6	27.5	57.9
$NiCo_2S_4$@300 °C	21.6	30.3	48.1
$NiCo_2S_4$@350 °C	24.0	29.1	46.9

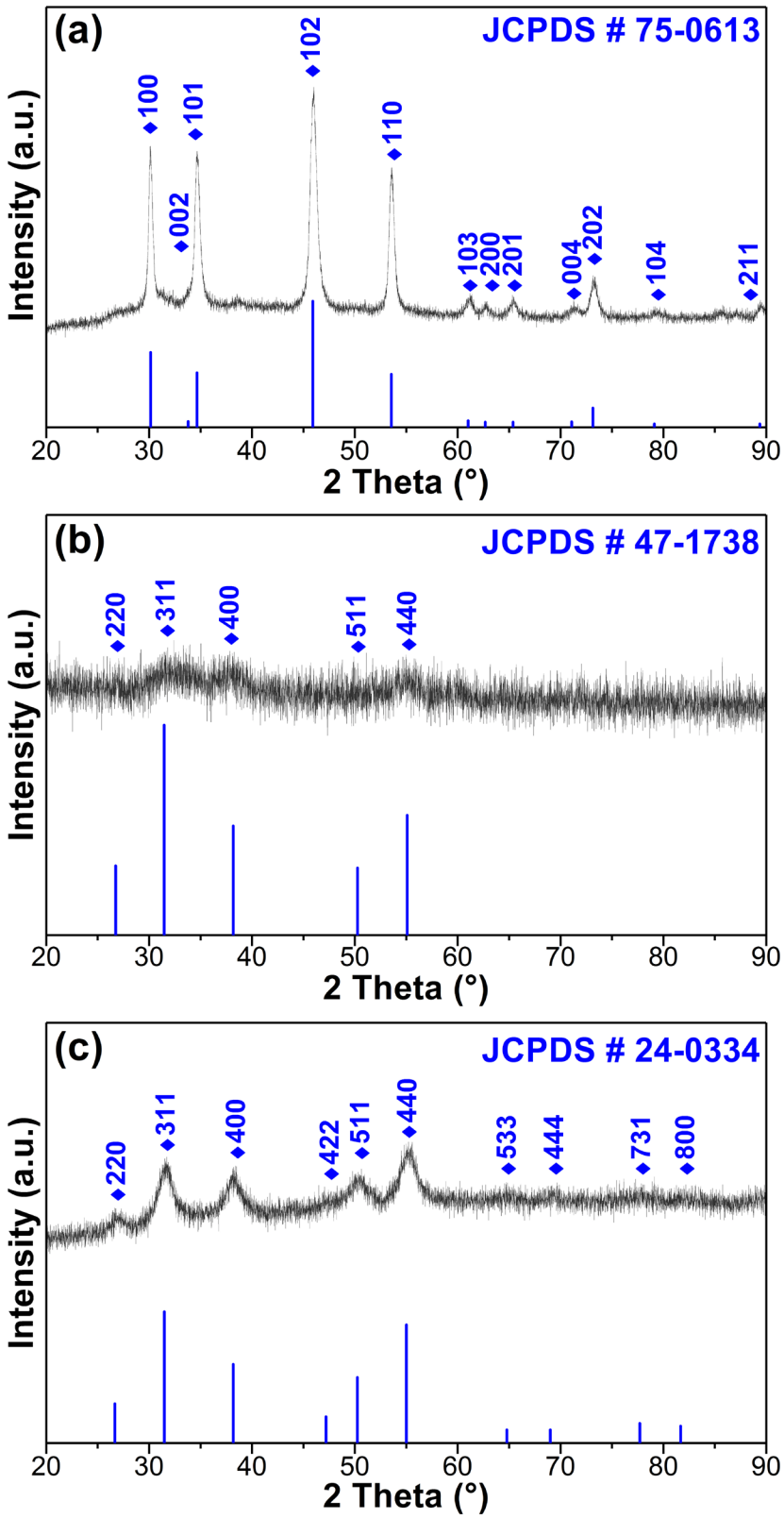

Figure S1. XRD patterns of the as-prepared (a) NiS, (b) Co_3S_4, and (c) $CoNi_2S_4$ NPs.

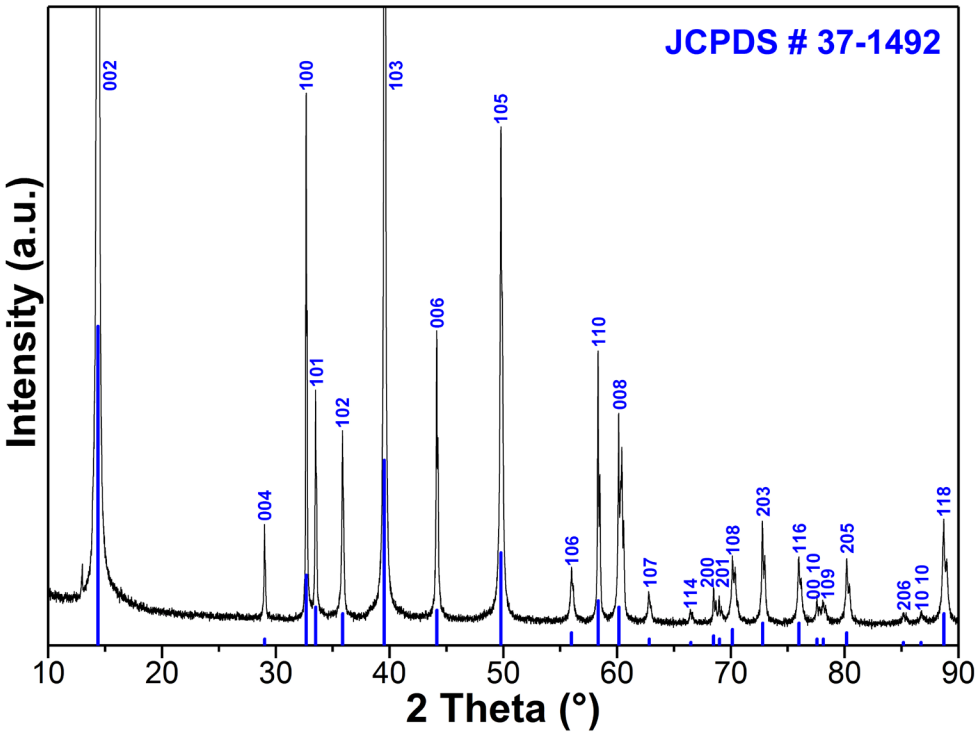

Figure S2. XRD patterns of the MoS_2 nanopowder. The characteristic peaks can be indexed to the hexagonal 2H–MoS_2 phase, corresponding to JCPDS No. 37-1492.

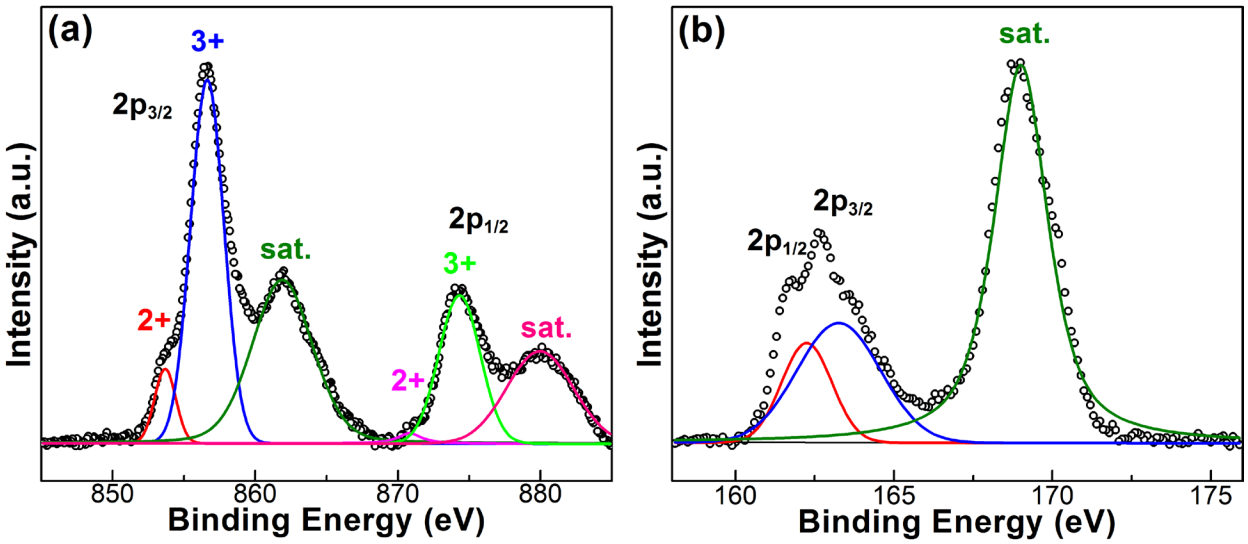

Figure S3. High-resolution XPS spectra of (a) Ni 2p and (b) S 2p regions for the as-prepared NiS.

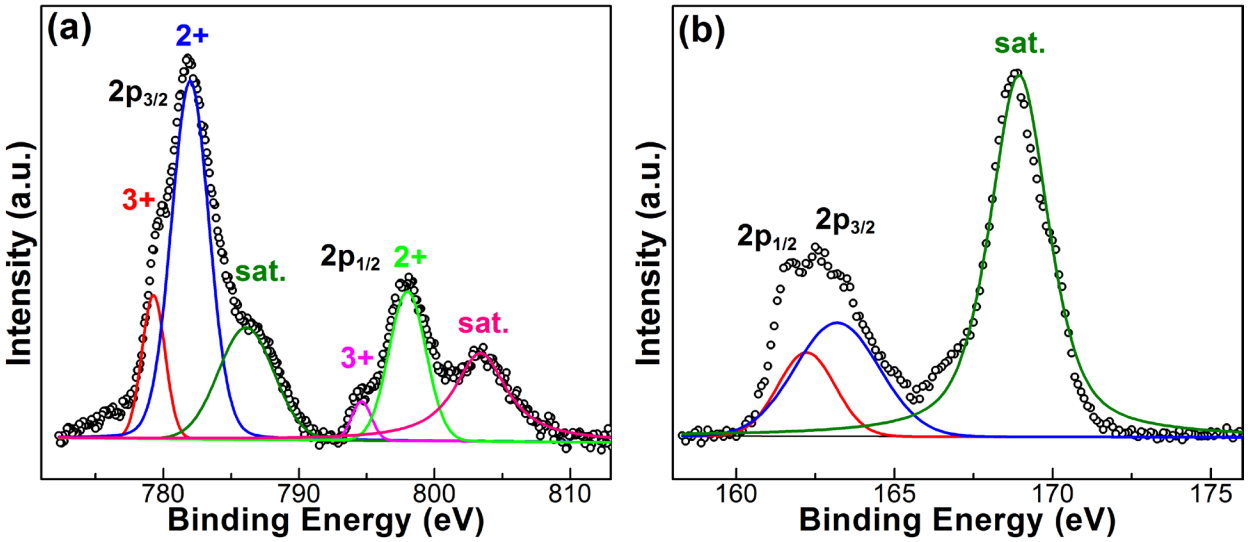

Figure S4. High-resolution XPS spectra of (a) Co 2p and (b) S 2p regions for the as-prepared Co_3S_4.

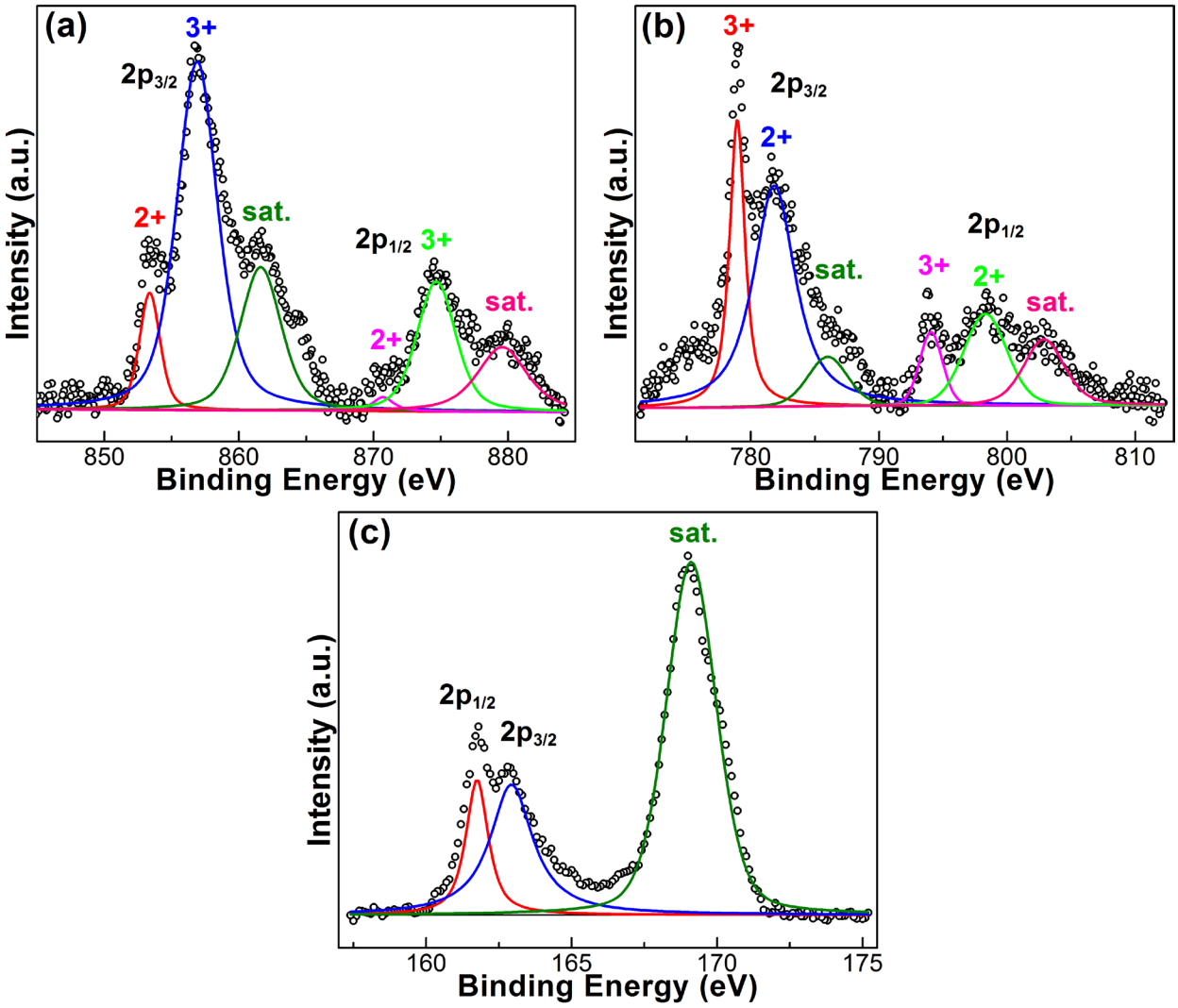

Figure S5. High-resolution XPS spectra of (a) Ni 2p, (b) Co 2p, and (c) S 2p regions for the as-prepared $CoNi_2S_4$.

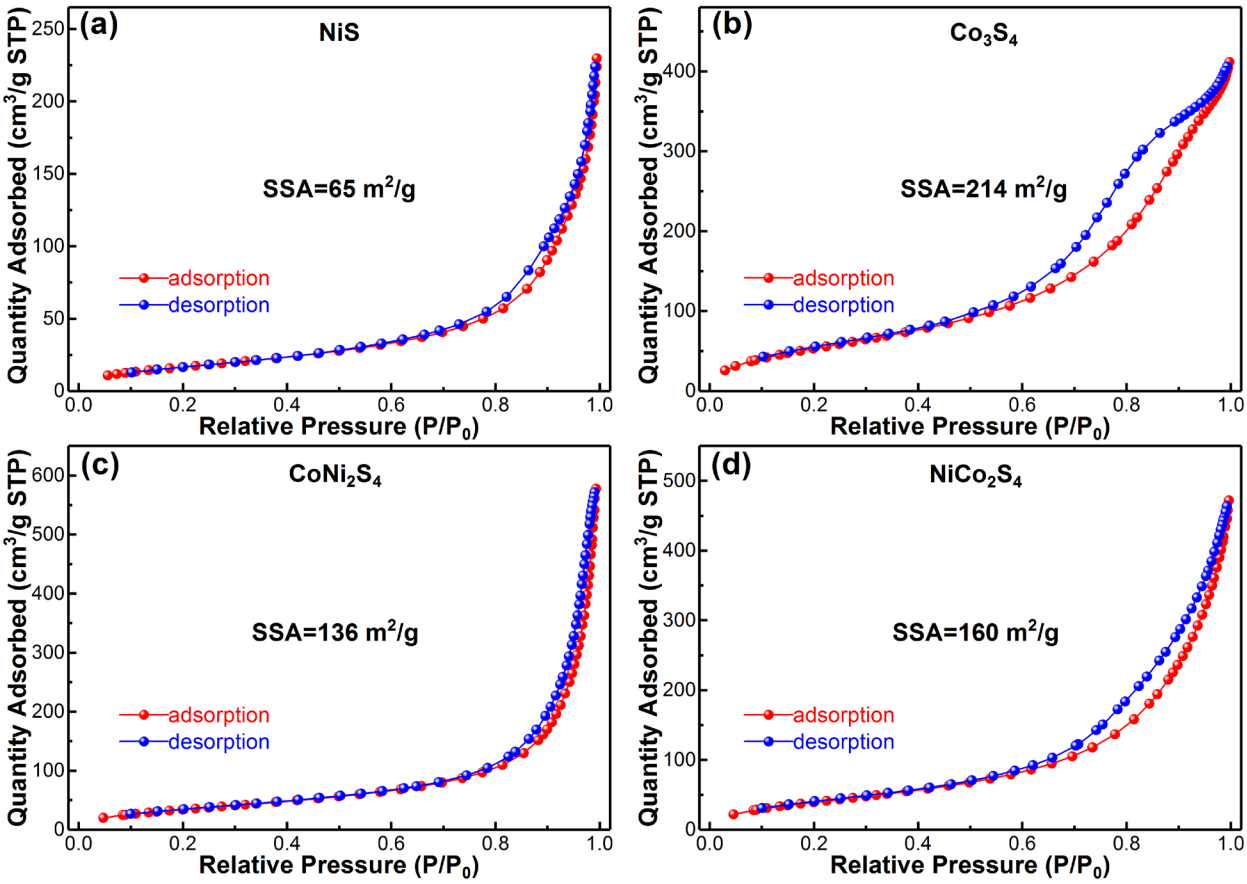

Figure S6. Nitrogen adsorption-desorption isotherms of (a) NiS, (b) Co_3S_4, (c) $CoNi_2S_4$ and (d) $NiCo_2S_4$ NPs, and their corresponding SSAs.

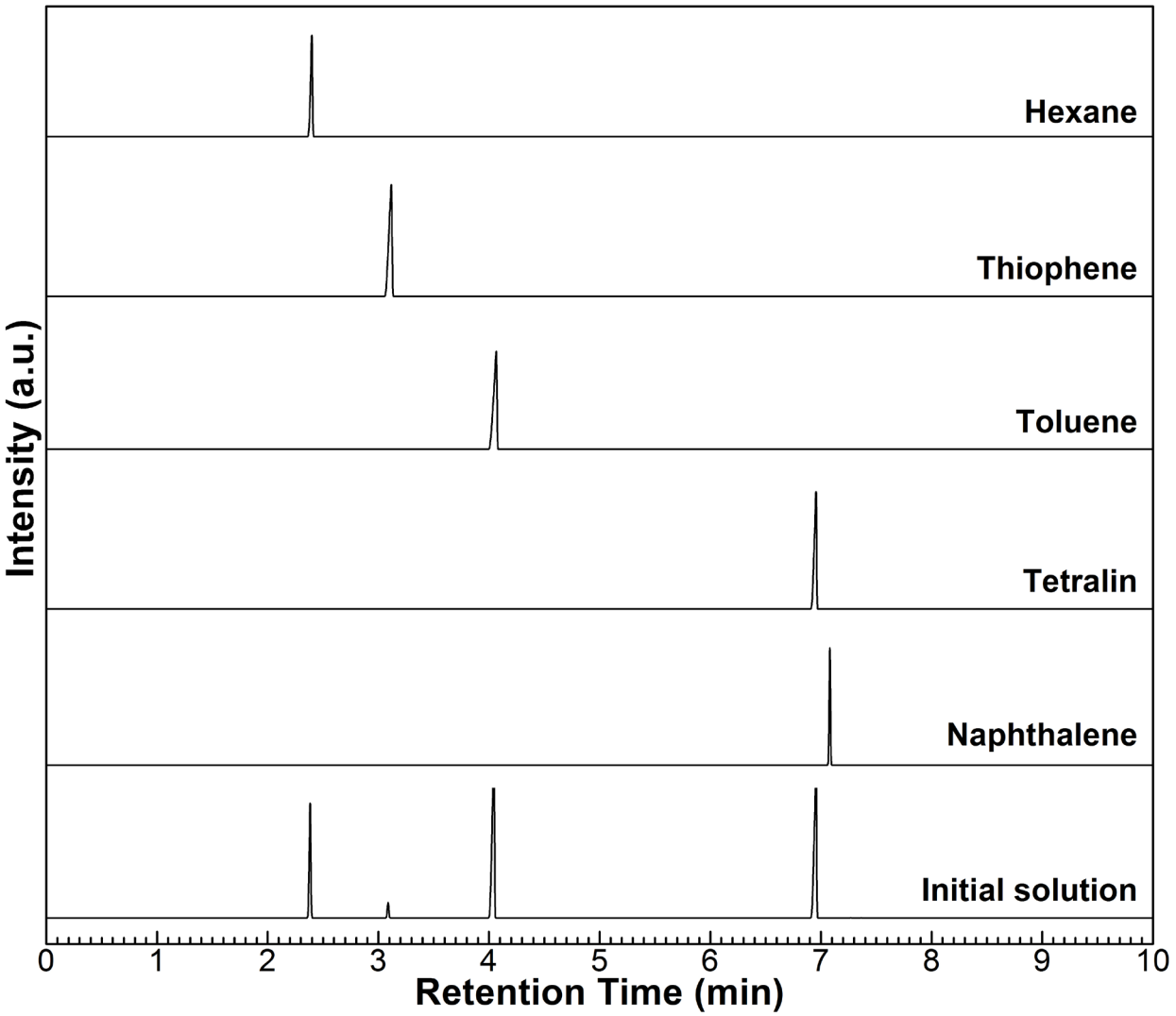

Figure S7. GC chromatograms for individual pure compound of hexane, thiophene, toluene, tetralin, and naphthalene, and for the initial mixture solution of hexane, thiophene and tetralin in toluene solvent.

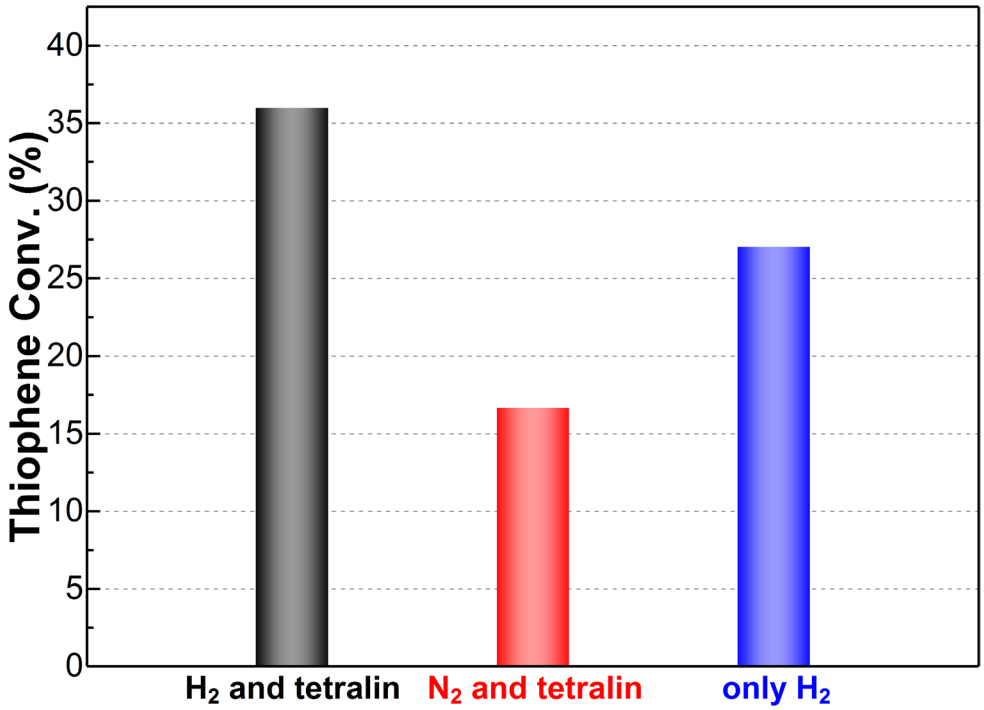

Figure S8. Thiophene conversion of the HDS reactions catalyzed with $NiCo_2S_4$ NPs at 340 °C for 5 h in the presence of hydrogen and tetralin, nitrogen and tetralin, and only hydrogen, respectively.

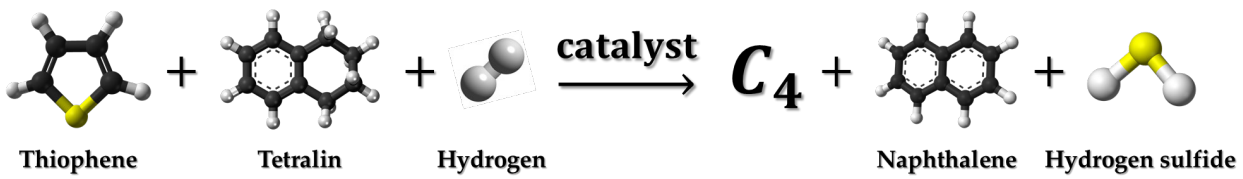

Figure S9. The main HDS reaction pathway illustrated by different molecules in 3-D ball model structure.

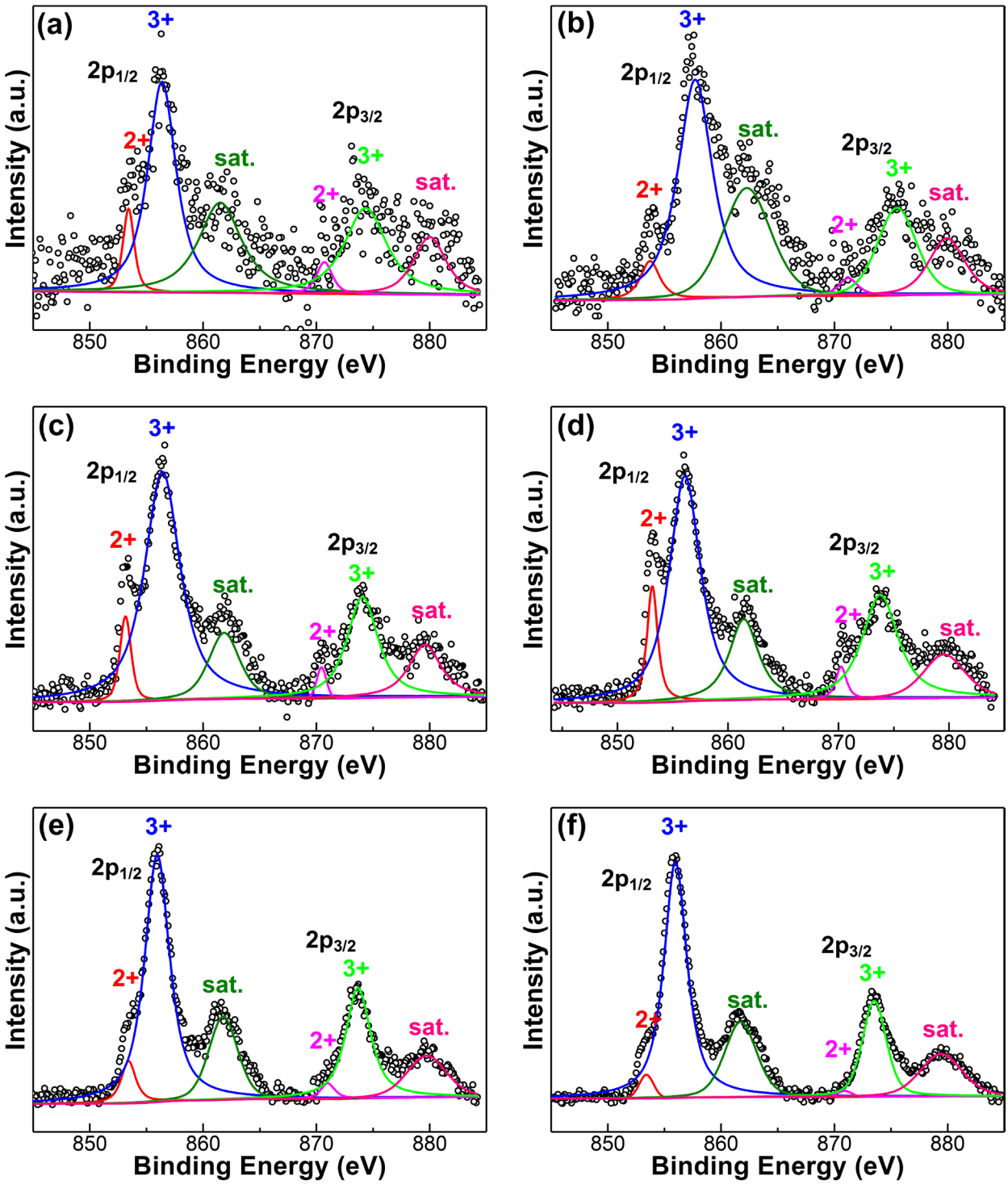

Figure S10. High-resolution XPS spectra of Ni 2p region for the $NiCo_2S_4$ prepared at (a) 180, (b) 200, (c) 230, (d) 250, (e) 300, and (f) 350 °C.

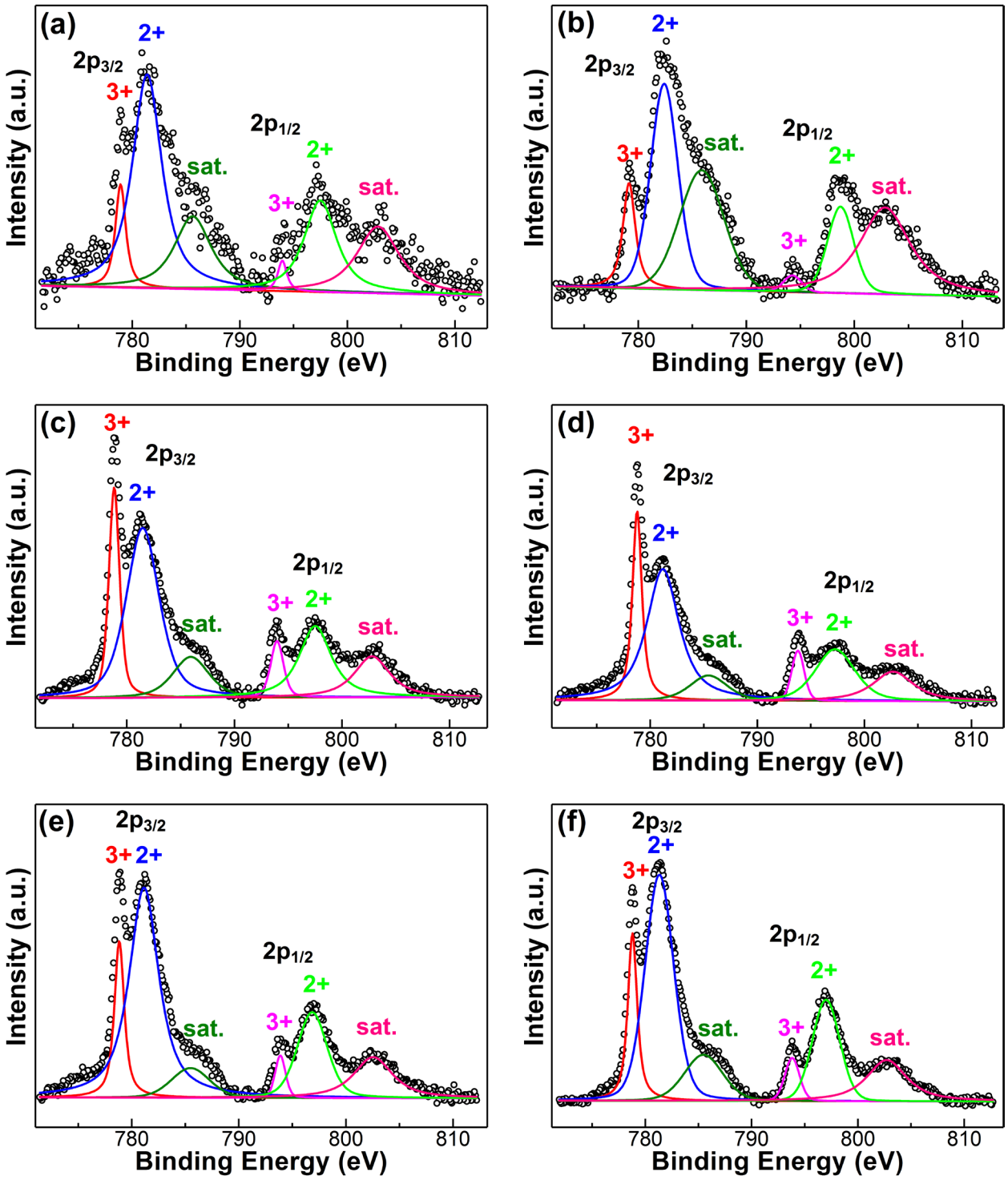

Figure S11. High-resolution XPS spectra of Co 2p region for the $NiCo_2S_4$ prepared at (a) 180, (b) 200, (c) 230, (d) 250, (e) 300, and (f) 350 °C.

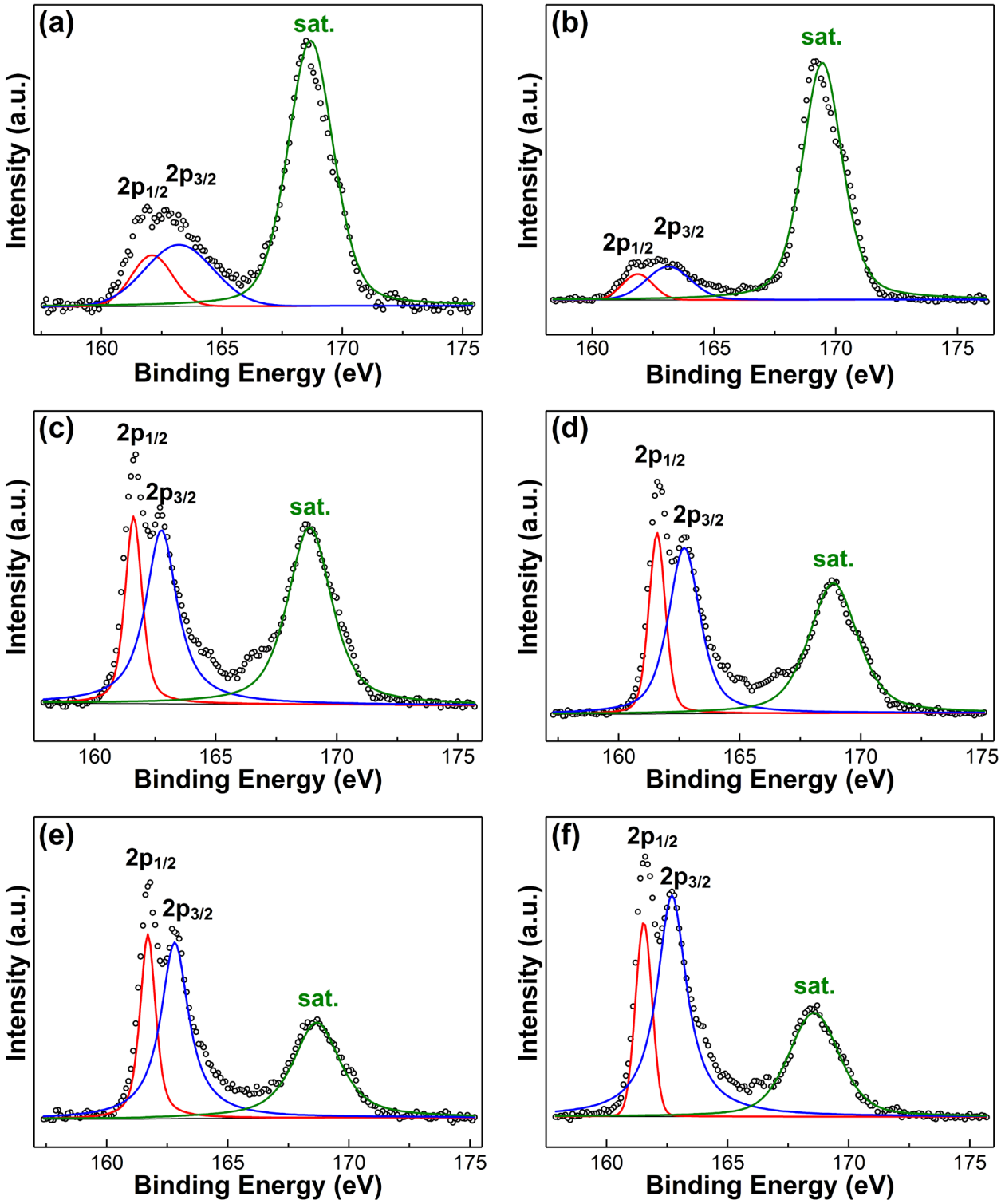

Figure S12. High-resolution XPS spectra of S 2p region for the $NiCo_2S_4$ prepared at (a) 180, (b) 200, (c) 230, (d) 250, (e) 300, and (f) 350 °C.

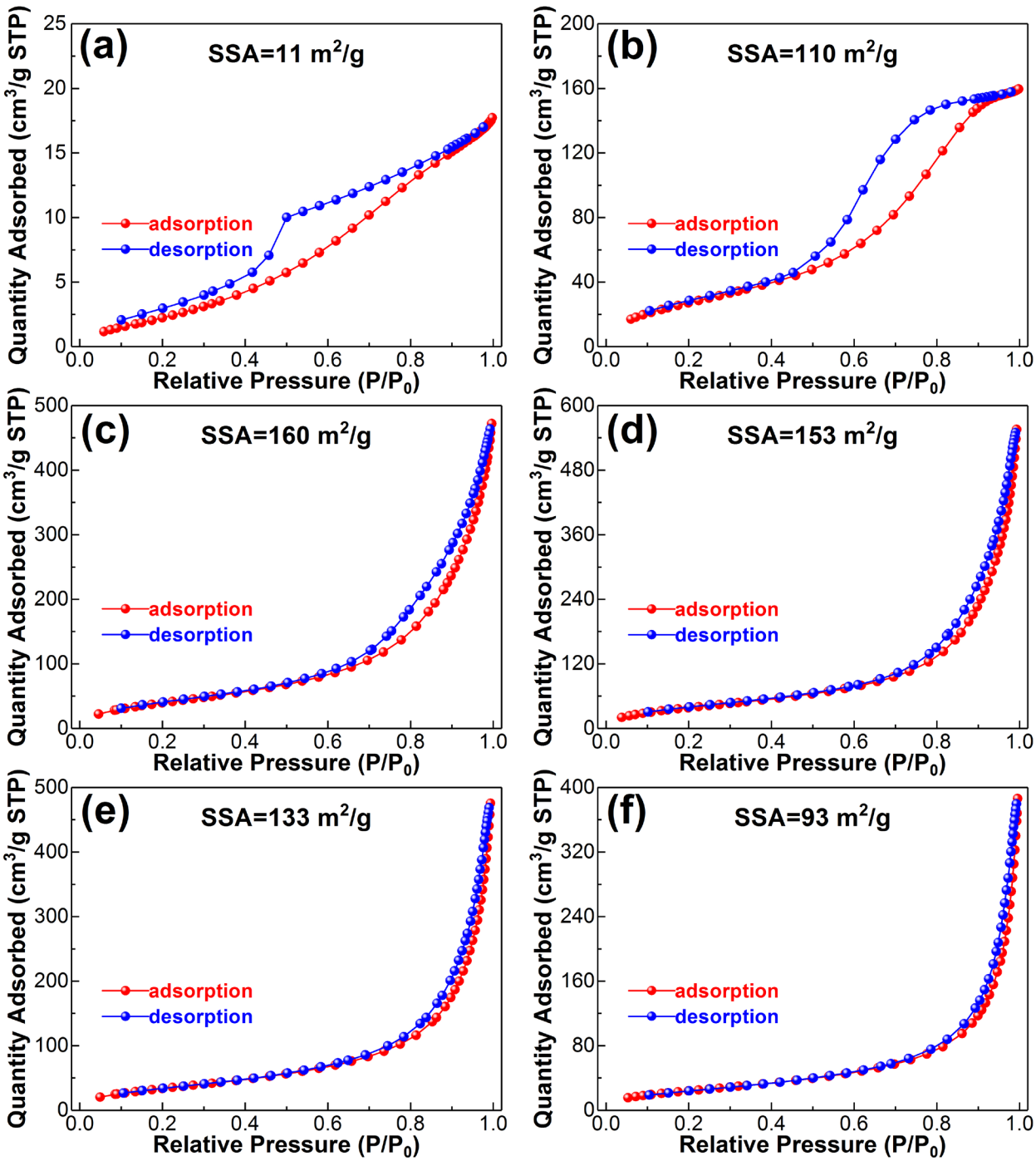

Figure S13. N_2 adsorption-desorption isotherms of the $NiCo_2S_4$ NPs prepared at different temperatures of (a) 180, (b) 200, (c) 230, (d) 250, (e) 300 and (f) 350 °C, and their corresponding SSAs.

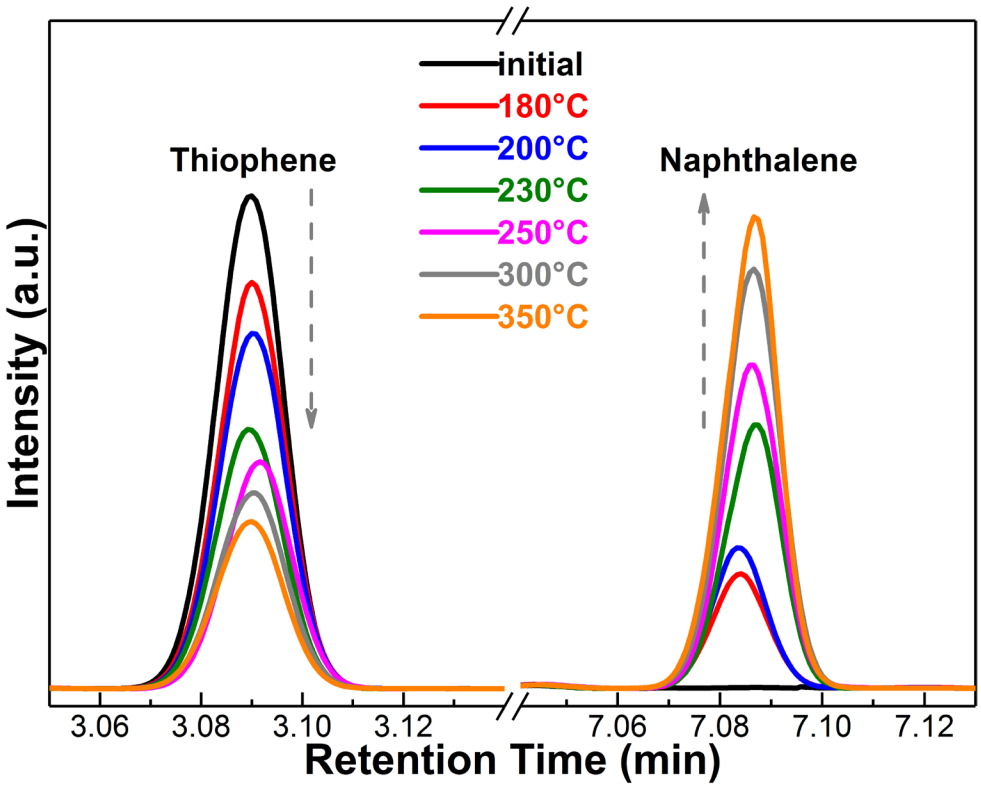

Figure S14. GC chromatograms for the thiophene and naphthalene compounds in the initial solution and in the HDS products catalyzed by $NiCo_2S_4$ prepared at six temperatures of 180, 200, 230, 250, 300, and 350 °C.

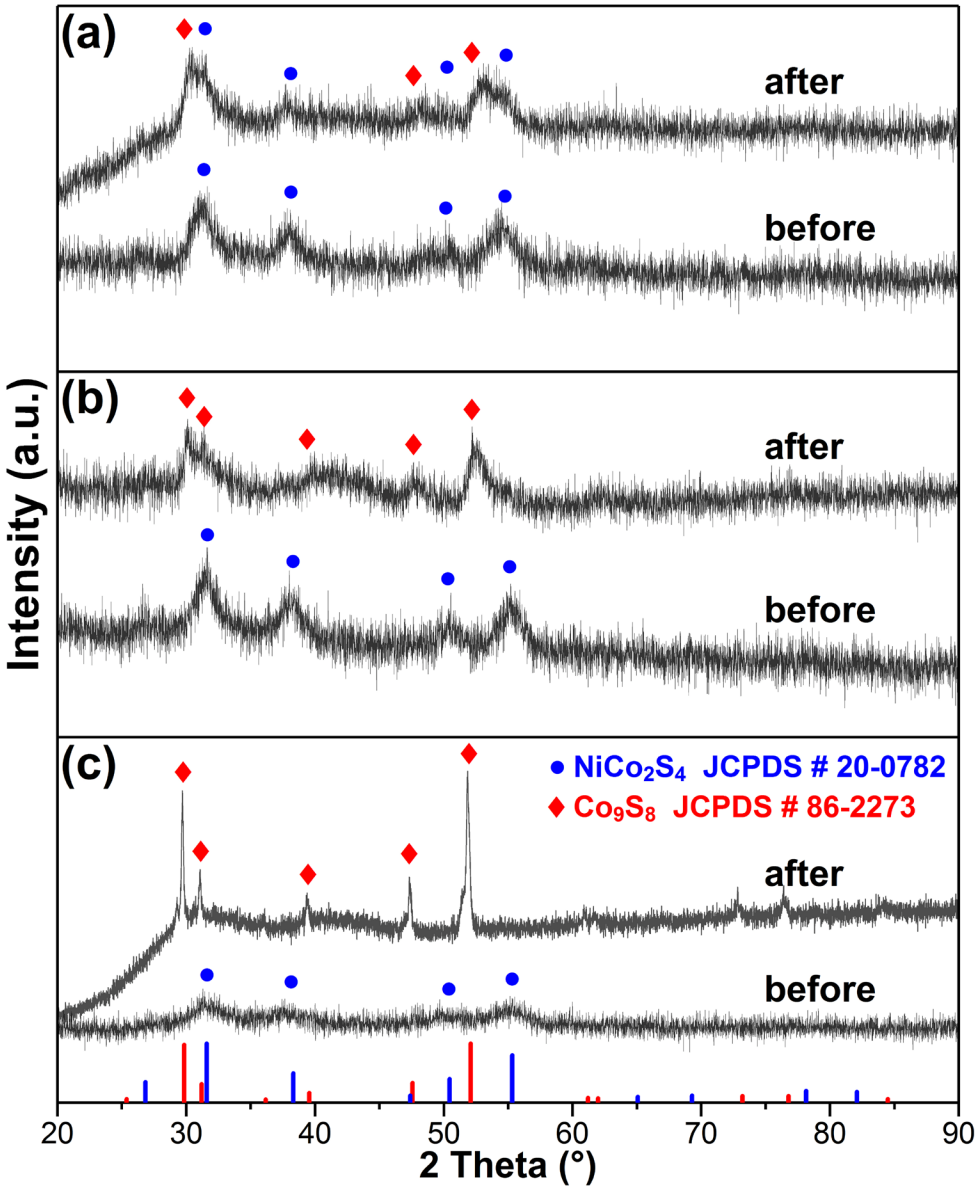

Figure S15. XRD patterns of the initial and spent $NiCo_2S_4$ catalysts prepared at 300 (a), 250 (b) and 200 (c) °C.